Optimal Preview Control for Automatic Carrier Landing System of Carrier-Based Aircraft with Air Wake

Li Meng[1], *Zhen Ziyang*[1*], *Gong Huajun*[1], *Hou Min*[1], *Huang Shuhong*[1]

1. College of Automation Engineering, Nanjing University of Aeronautics and Astronautics, Nanjing 211106, P. R. China

(Received 1 July 2016; revised 2 November 2016; accepted 9 February 2017)

Abstract: Carrier-based aircraft carrier landing is a special kind of tracking control problem and not suitable for classical control methods, which may miss the desired performance or result in overdesign. Therefore, we present an optimal preview control for automatic carrier landing system (ACLS) by using state information of system, as well as future reference information, which can avoid the shortcomings of classical control methods. Since the flight performance of carrier-based aircraft is disturbed by air wake when the aircraft flies near the area of carrier stern, we design a disturbance rejection strategy to ensure that aircraft track the glide path with high precision and robustness. Further, carrier-based aircraft is a complex nonlinear system. However, the nonlinear model of carrier-based aircraft can be linearized at equilibrium landing state and decoupled into the longitudinal model and the lateral model. Therefore, an optimal preview control system is designed. The simulation results of a carrier-based aircraft show that the optimal preview control system can effectively suppress air wake. Tracking accuracy of optimal preview controller is higher than that of the proportional integral differential (PID) control system.

Key words: carrier-based aircraft; carrier landing; optimal control; preview control; nonlinear model

CLC number: V249.1 **Document code**: A **Article ID**: 1005-1120(2017)06-0659-10

0 Introduction

Carrier-based aircraft plays an increasingly important role in modern wars. Statistics show that eight accidents of carrier-based aircraft in ten occur in landing process since the process is more difficult and complicated than others[1]. Therefore, it is crucial to research features of carrier-based aircraft carrier landing. Automatic carrier landing system (ACLS) can improve the safety of carrier-based aircraft in carrier landing and reduce burdens on the pilots. Carrier landing control law is the core of ACLS. At present, proportional integral differential (PID) controller has been applied to ACLS[2]. Carrier landing performance of F14 carrier-based aircraft was improved by the direct lift control[3], which synthesized state-feedback controller for aerospace and marine applications[4-5]. Discrete variable structure control theory was developed based on disturbance compensation[6]. However, in practice, PID controller can hardly guide carrier-based aircraft to track reference glide path perfectly. The damping force of carrier-based aircraft when landing, as well as the height, must be considered[7]. Aircraft carrier landing is complex, usually influenced by a combination of pilot physical conditions, external environments and equipment performances[8], and current practical approaches cannot completely satisfy its requirements of high accuracy and robustness. Therefore, an efficient control method is required.

Optimal preview control theory uses information not only in past and at present but also in the future. Therefore, it can greatly improve tracking performance of closed loop system, holding better tracking precision, higher robustness and faster response speed than PID control.

* Corresponding author, E-mail address: zhenziyang@nuaa.edu.cn.

How to cite this article: Li Meng, Zhen Ziyang, Gong Huajun, et al. Optimal preview control for automatic carrier landing system of carrier-based aircraft with air wake[J]. Trans. Nanjing Univ. Aero. Astro., 2017,34(6):659-668.
http://dx.doi.org/10.16356/j.1005-1120.2017.06.659

Ref. [9] presented three methods to solve optimal servo system, namely partial differential optimization method, extended error system method and successive optimization method. Ref. [10] facilitated optimal preview controller in thermal power unit and achieved preferable results[10]. Zhen[11-12] proposed an optimal preview control method based on information fusion of error system and obtained high tracking accuracy. He[13] subsequently described the theory and application of the preview control. Optimal preview control theory has a broad prospect in many fields.

Therefore, we design an optimal preview control system based on the mathematical model of carrier-based aircraft in carrier landing phase. The optimal preview control system utilizes not only state feedback information, system model information and performance index information, but also the previewed glide path information, which is not utilized in the traditional carrier landing systems[14]. Different from previous study [15], we present a disturbance rejection strategy of the air wake to ensure that aircraft track the reference glide path with high precision and robustness under the interference of the air wake.

1 Carrier Landing Problem Description

The longitudinal ACLS and the lateral ACLS are developed to ensure carrier-based aircraft quickly and accurately track reference glide path and fly along deck center line. The longitudinal ACLS consists of a pitch attitude controller, an approach power compensation controller and a altitude controller. The lateral ACLS consists of a roll attitude controller, a heading controller and a lateral deviation controller. The mathematical model of carrier-based aircraft is a multiple input multiple output (MIMO) control system, thus classical control method may be not reliable and even come to the wrong conclusion in analysis of MIMO system. Optimal preview control theory is effective to deal with the system.

1.1 Carrier-based aircraft dynamics equation

The nonlinear dynamic models of a six degree-of-freedom carrier-based aircraft are presented based on the body axes coordinate system. The dynamic equations are as follows

(1) Force equations

$$\begin{cases}\dot{u}=vr-wq-g\sin\theta+\dfrac{F_x}{m}\\ \dot{v}=-ur+wp+g\cos\theta\sin\varphi+\dfrac{F_y}{m}\\ \dot{w}=uq-vp+g\cos\theta\cos\varphi+\dfrac{F_z}{m}\end{cases}\tag{1}$$

(2) Moment equations

$$\begin{cases}\dot{p}=(c_1r+c_2p)q+c_3\bar{L}+c_4N\\ \dot{q}=c_5pr-c_6(p^2-r^2)+c_7M\\ \dot{r}=(c_8p-c_2r)q+c_4\bar{L}+c_9N\end{cases}\tag{2}$$

where $c_1=\dfrac{(I_y-I_z)I_z-I_{xz}^2}{I_xI_z-I_{xz}^2}$, $c_2=\dfrac{(I_x-I_y+I_z)I_{xz}}{I_xI_z-I_{xz}^2}$, $c_3=\dfrac{I_z}{I_xI_z-I_{xz}^2}$, $c_4=\dfrac{I_{xz}}{I_xI_z-I_{xz}^2}$, $c_5=\dfrac{I_z-I_x}{I_y}$, $c_6=\dfrac{I_{xz}}{I_y}$, $c_7=\dfrac{1}{I_y}$, $c_8=\dfrac{I_x(I_x-I_y)+I_{xz}^2}{I_xI_z-I_{xz}^2}$, $c_9=\dfrac{I_x}{I_xI_z-I_{xz}^2}$.

(3) Kinematic equations

$$\begin{cases}\dot{\varphi}=p+(r\cos\varphi+q\sin\varphi)\tan\theta\\ \dot{\theta}=q\cos\varphi-r\sin\varphi\\ \dot{\psi}=\dfrac{1}{\cos\theta}(r\cos\varphi+q\sin\varphi)\end{cases}\tag{3}$$

(4) Navigation equations

$$\begin{cases}\dot{x}_g=V\cos\mu\cos\varphi\\ \dot{y}_g=V\cos\mu\sin\varphi\\ \dot{h}=V\sin\mu\end{cases}\tag{4}$$

Based on Eqs. (1)—(4) and aerodynamic parameters of F18 carrier-based aircraft, nonlinear model is established by S function in MATLAB.

Since nonlinear design strategy is complicated, linear state space equations can be obtained based on flight characteristics of landing phase

$$\dot{\boldsymbol{x}}=\boldsymbol{A}\boldsymbol{x}+\boldsymbol{B}\boldsymbol{u}\tag{5}$$

where $\boldsymbol{x}=[\Delta V\quad \Delta\alpha\quad \Delta q\quad \Delta\theta\quad \Delta\beta\quad \Delta p\quad \Delta r\quad \Delta\varphi\quad \Delta\psi]^{\mathrm{T}}$ are state variables including the speed, the angle of attack, the pitch rate, the pitch angle, the side slip angle, the roll rate, the yaw rate, the roll angle and the yaw angle, $\boldsymbol{u}=[\delta_e\quad \delta_T\quad \delta_a$

$\delta_r]^{\mathrm{T}}$ are control surface inputs, respectively denoting elevator angle, throttle lever, aileron angle and rudder angle.

Linear equations of small disturbance of the longitudinal dynamics with height and the lateral dynamics with lateral deviation are described as[16]

$$\dot{\boldsymbol{x}}_{\mathrm{lon}} = \boldsymbol{A}_{\mathrm{lon}} \boldsymbol{x}_{\mathrm{lon}} + \boldsymbol{B}_{\mathrm{lon}} \boldsymbol{u}_{\mathrm{lon}} \tag{6}$$

$$\dot{\boldsymbol{x}}_{\mathrm{lat}} = \boldsymbol{A}_{\mathrm{lat}} \boldsymbol{x}_{\mathrm{lat}} + \boldsymbol{B}_{\mathrm{lat}} \boldsymbol{u}_{\mathrm{lat}} \tag{7}$$

where $\boldsymbol{x}_{\mathrm{lon}} = [\Delta V \quad \Delta\alpha \quad \Delta q \quad \Delta\theta \quad \Delta h]^{\mathrm{T}}$, $\boldsymbol{x}_{\mathrm{lat}} = [\Delta\beta \quad \Delta p \quad \Delta r \quad \Delta\varphi \quad \Delta\psi \quad \Delta y_{\mathrm{lat}}]^{\mathrm{T}}$, $\boldsymbol{u}_{\mathrm{lon}} = [\Delta\delta_e \quad \Delta\delta_T]^{\mathrm{T}}$, $\boldsymbol{u}_{\mathrm{lat}} = [\Delta\delta_a \quad \Delta\delta_r]^{\mathrm{T}}$, $\boldsymbol{A}_{\mathrm{lon}} =$

$$\begin{bmatrix} -0.0895 & 3.3703 & -0.0254 & -32.1112 & 0 \\ -0.0012 & -0.5871 & 0.9908 & 0.0085 & 0 \\ 0 & -0.3001 & -0.1845 & 0 & 0 \\ 0 & 0 & 1 & 0 & 0 \\ 0 & -70/0.3048 & 0 & 70/0.3048 & 0 \end{bmatrix},$$

$$\boldsymbol{B}_{\mathrm{lon}} = \begin{bmatrix} -0.0045 & 18.8037 \\ -0.0014 & -0.0123 \\ -0.0260 & 0 \\ 0 & 0 \\ 0 & 0 \end{bmatrix}, \quad \boldsymbol{A}_{\mathrm{lat}} =$$

$$\begin{bmatrix} -0.1035 & 0.1474 & -0.9872 & 0.1410 & 0 & 0 \\ -4.0684 & -1.2514 & 0.5846 & 0 & 0 & 0 \\ 0.5583 & -0.0090 & -0.0791 & 0 & 0 & 0 \\ 0 & 1.0000 & 0.0875 & 0 & 0 & 0 \\ 0 & 0 & 1.0038 & 0 & 0 & 0 \\ 0 & 0 & 0 & 0 & 70/0.3048 & 0 \end{bmatrix},$$

$$\boldsymbol{B}_{\mathrm{lat}} = \begin{bmatrix} 0 & 0.0004 \\ 0.0470 & 0.0074 \\ -0.0007 & -0.0058 \\ 0 & 0 \\ 0 & 0 \\ 0 & 0 \end{bmatrix}.$$

1.2 Air wake description

In the carrier landing process, the maximum height error is caused by air wake. It is a norm that longitudinal height error of ideal carrier landing point should be controlled within 12.2 m. Only one of the air wake component can cause 39 m longitudinal height error without taking air wake rejection technique[17].

Aircraft will be affected by air wake when the distance between the aircraft and the aircraft carrier is less than 800 m. Generally, air wake consist of four parts.

(1) Free atmospheric turbulence components: u_1, v_1, w_1;

(2) Steady state components: u_2, w_2;

(3) Periodic components: u_3, w_3;

(4) Random components: u_4, v_4, w_4.

There is

$$\begin{cases} u_g = u_1 + u_2 + u_3 + u_4 \\ v_g = v_1 + v_4 \\ w_g = w_1 + w_2 + w_3 + w_4 \end{cases} \tag{8}$$

where u_g denotes the horizontal wake, v_g the transverse wake and w_g the longitudinal wake.

We add Eq. (8) into Eqs. (6), (7), then linear equations of longitudinal channel and lateral channel with air wake become[16]

$$\dot{\boldsymbol{x}}_{\mathrm{lon}} = \boldsymbol{A}_{\mathrm{lon}} \boldsymbol{x}_{\mathrm{lon}} + \boldsymbol{B}_{\mathrm{lon}} \boldsymbol{u}_{\mathrm{lon}} + \boldsymbol{E}_{\mathrm{lon}} \boldsymbol{d}_{\mathrm{lon}} \tag{9}$$

$$\dot{\boldsymbol{x}}_{\mathrm{lat}} = \boldsymbol{A}_{\mathrm{lat}} \boldsymbol{x}_{\mathrm{lat}} + \boldsymbol{B}_{\mathrm{lat}} \boldsymbol{u}_{\mathrm{lat}} + \boldsymbol{E}_{\mathrm{lat}} \boldsymbol{d}_{\mathrm{lat}} \tag{10}$$

where $\boldsymbol{E}_{\mathrm{lon}} = \begin{bmatrix} 0 \\ 0 \\ 0 \\ 0 \\ 1/0.3048 \end{bmatrix}$, $\boldsymbol{E}_{\mathrm{lat}} = \begin{bmatrix} 0 \\ 0 \\ 0 \\ 0 \\ 0 \\ 1/0.3048 \end{bmatrix}$.

1.3 Carrier landing control problem description

The carrier-based aircraft landing process is extremely complicated and risky. However, ACLS can completely solve the problem. The core of ACLS is flight control system, as shown in Fig. 1.

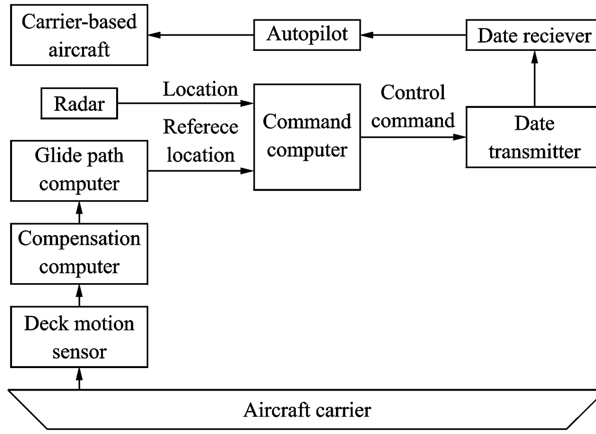

Fig. 1 ACLS principle

Location of carrier-based aircraft and deck motion of aircraft carrier are measured by tracking radar equipped on the carrier. The reference location of the aircraft can be calculated based on the deck motion. The location and reference location of the aircraft are input into command computer to obtain control command of error signal. Then the aircraft receives these control commands by data link. Finally, the aircraft′s autopilots can eliminate the error and land the aircraft at the predetermined location. Here, the reference glide path is a three dimensional route or to be specific, this path is a two dimensional path when the aircraft flied along the deck center line with an initial height of 240 m, an initial speed of 70 m/s and an initial glide angle of 3.5°. However, air wake must be considered before 12.5 s of the landing.

2 Optimal Preview Control Based ACLS

2.1 Optimal preview control scheme

The reference glide path is greatly important for the design of optimal preview control system. The basic idea of optimal preview control theory is to achieve minimal evaluation function value and achieve excellent pole placement. In order to maintain stability of state variables, optimal preview controller leads the deviation of state variables to converge to zero. In particular application, however, this control input is not the best. Therefore, mathematical model of carrier-based aircraft carrier landing can be deduced to the expanding system based on error signal.

Optimal preview control is a new engineering realization method. It takes the full use of future reference information as a feed forward input. The feed forward input can be varied with reference information, which can greatly improve tracking performance of the control system. The optimal preview control system is shown in Fig. 2.

Optimal preview control system faciliatates the past, the present and the future information

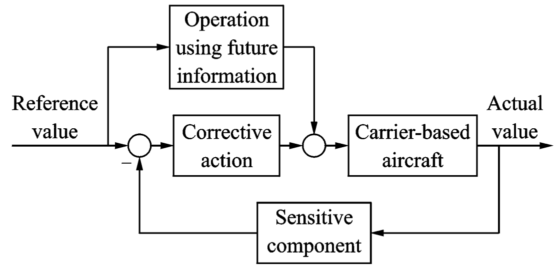

Fig. 2 Optimal preview control system

for analysis and comprehensive control. This system has the following advantages.

(1) It can perform operation for object in advance, so instant energy consumption is relatively small.

(2) It can determine whether current operation is right or wrong in a long run, and avoid unreasonable decisions as much as possible.

(3) It can make a decision as soon as possible so as to improve system response speed.

2.2 Longitudinal channel optimal preview control scheme

Reference height of carrier-based aircraft changes with time in the longitudinal channel, and is influenced by air wake. The discrete mathematical equations of carrier-based aircraft longitudinal channel are obtained

$$\boldsymbol{x}_{\text{lon}}(k+1)=\boldsymbol{A}_{\text{lon}}\boldsymbol{x}_{\text{lon}}(k)+\boldsymbol{B}_{\text{lon}}\boldsymbol{u}_{\text{lon}}(k)+\boldsymbol{E}_{\text{lon}}\boldsymbol{d}_{\text{lon}}(k)$$
$$\boldsymbol{y}_{\text{lon}}(k)=\boldsymbol{C}_{\text{lon}}\boldsymbol{x}_{\text{lon}}(k) \tag{11}$$

where $\boldsymbol{A}_{\text{lon}}$, $\boldsymbol{B}_{\text{lon}}$, $\boldsymbol{C}_{\text{lon}}$, $\boldsymbol{E}_{\text{lon}}$ are corresponding dimension matrix.

Aiming at the discrete equations, error signal term can be expressed as

$$\boldsymbol{e}_{\text{lon}}(k)=\boldsymbol{R}_{\text{lon}}(k)-\boldsymbol{y}_{\text{lon}}(k) \tag{12}$$

where $\boldsymbol{y}_{\text{lon}}$ is longitudinal output signal and $\boldsymbol{R}_{\text{lon}}$ the reference value of $\boldsymbol{y}_{\text{lon}}$.

Substitue the error signal in Eq. (12) into Eq. (11), a new state space equation can be obtained

$$\begin{bmatrix}\boldsymbol{e}_{\text{lon}}(k+1)\\ \Delta\boldsymbol{x}_{\text{lon}}(k+1)\end{bmatrix}=\begin{bmatrix}\boldsymbol{I}_{\text{lon}} & -\boldsymbol{C}_{\text{lon}}\boldsymbol{A}_{\text{lon}}\\ 0 & \boldsymbol{A}_{\text{lon}}\end{bmatrix}\begin{bmatrix}\boldsymbol{e}_{\text{lon}}(k)\\ \Delta\boldsymbol{x}_{\text{lon}}(k)\end{bmatrix}+\begin{bmatrix}-\boldsymbol{C}_{\text{lon}}\boldsymbol{B}_{\text{lon}}\\ \boldsymbol{B}_{\text{lon}}\end{bmatrix}\Delta\boldsymbol{u}_{\text{lon}}(k)+\begin{bmatrix}\boldsymbol{I}_m\\ 0\end{bmatrix}\Delta\boldsymbol{R}_{\text{lon}}(k+1)+\begin{bmatrix}-\boldsymbol{C}_{\text{lon}}\boldsymbol{E}_{\text{lon}}\\ \boldsymbol{E}_{\text{lon}}\end{bmatrix}\Delta\boldsymbol{d}_{\text{lon}}(k) \tag{13}$$

namely

$$\boldsymbol{X}_{\text{lon}}(k+1)=\boldsymbol{\Phi}_{\text{lon}}\boldsymbol{X}_{\text{lon}}(k)+\boldsymbol{G}_{\text{lon}}\boldsymbol{U}_{\text{lon}}(k)+\boldsymbol{G}_{R\text{lon}}\boldsymbol{R}_{\text{lon}}(k+1)+\boldsymbol{G}_{d\text{lon}}\boldsymbol{D}_{\text{lon}}(k) \tag{14}$$

The quadratic form evaluation function of the error term and the input term can be expressed as

$$\boldsymbol{J}_{\text{lon}}=\sum_{k=-M+1}^{\infty}\left[\boldsymbol{X}_{\text{lon}}^{\text{T}}(k)\boldsymbol{Q}_{\text{lon}}\boldsymbol{X}_{\text{lon}}(k)+\boldsymbol{U}_{\text{lon}}^{\text{T}}(k)\boldsymbol{H}_{\text{lon}}\boldsymbol{U}_{\text{lon}}(k)\right] \tag{15}$$

where $\boldsymbol{Q}_{\text{lon}}$ is a semi positive definite matrix, $\boldsymbol{H}_{\text{lon}}$ a positive definite matrix and M is the larger value of M_R and M_d. Eq. (15) is summation from $-M+1$ to ∞. Target value changes in $k=1$, and the input value begins to change before M steps at this time. This time is not the absolute physical moment, but the relative moment.

Considering the change of reference information and disturbance information, optimal preview control inputs can minimize the evaluation function value. First of all, the form of control law is assumed, and put into the evaluation function to calculate evaluation function value. Finally, preview feed forward coefficient and optimal feedback coefficient are gained. This method is called partial differential optimization method[9].

Target value is known, which starts from current time until the next M_R steps. And disturbance value is also known, which starts from current time until the next M_d steps. Optimal preview control law is obtained

$$\Delta\boldsymbol{u}_{\text{lon}}(k)=\boldsymbol{F}_{k\text{lon}}\boldsymbol{X}_{\text{lon}}(k)+\sum_{j=0}^{M_R}\boldsymbol{F}_{R\text{lon}}(j)\Delta\boldsymbol{R}_{\text{lon}}(k+j)+\sum_{j=0}^{M_d}\boldsymbol{F}_{d\text{lon}}(j)\Delta\boldsymbol{d}_{\text{lon}}(k+j) \tag{16}$$

The full state feedback coefficient is obtained based on optimal preview control algorithm of the longitudinal channel of carrier-based aircraft.

$$\boldsymbol{F}_{k\text{lon}}=-\left[\boldsymbol{H}_{\text{lon}}+\boldsymbol{G}_{\text{lon}}^{\text{T}}\boldsymbol{P}_{\text{lon}}\boldsymbol{G}_{\text{lon}}\right]^{-1}\boldsymbol{G}_{\text{lon}}^{\text{T}}\boldsymbol{P}_{\text{lon}}\boldsymbol{\Phi}_{\text{lon}} \tag{17}$$

where

$$\boldsymbol{P}_{\text{lon}}=\boldsymbol{Q}_{\text{lon}}+\boldsymbol{\Phi}_{\text{lon}}^{\text{T}}\boldsymbol{P}_{\text{lon}}\boldsymbol{\Phi}_{\text{lon}}-\boldsymbol{\Phi}_{\text{lon}}^{\text{T}}\boldsymbol{P}_{\text{lon}}\boldsymbol{G}_{\text{lon}}\left[\boldsymbol{H}_{\text{lon}}+\boldsymbol{G}_{\text{lon}}^{\text{T}}\boldsymbol{P}_{\text{lon}}\boldsymbol{G}_{\text{lon}}\right]^{-1}\boldsymbol{G}_{\text{lon}}^{\text{T}}\boldsymbol{P}_{\text{lon}}\boldsymbol{\Phi}_{\text{lon}} \tag{18}$$

The optimal preview feed forward coefficient $\boldsymbol{F}_{R\text{lon}}$ and $\boldsymbol{F}_{d\text{lon}}$ are obtained based on the partial differential optimization method. The target feed forward coefficient and disturbance feed forward coefficient can be expressed as

$$\begin{cases}\boldsymbol{F}_{R\text{lon}}(j)=0 & j=0\\ \boldsymbol{F}_{R\text{lon}}(j)=-\left[\boldsymbol{H}_{\text{lon}}+\boldsymbol{G}_{\text{lon}}^{\text{T}}\boldsymbol{P}_{\text{lon}}\boldsymbol{G}_{\text{lon}}\right]^{-1} * \\ \quad \boldsymbol{G}_{\text{lon}}^{\text{T}}(\boldsymbol{\xi}_{\text{lon}}^{\text{T}})^{j-1}\boldsymbol{P}_{\text{lon}}\boldsymbol{G}_{R\text{lon}} & j\geqslant 1\end{cases} \tag{19}$$

$$\boldsymbol{F}_{d\text{lon}}(j)=-\left[\boldsymbol{H}_{\text{lon}}+\boldsymbol{G}_{\text{lon}}^{\text{T}}\boldsymbol{P}_{\text{lon}}\boldsymbol{G}_{\text{lon}}\right]^{-1} * \boldsymbol{G}_{\text{lon}}^{\text{T}}(\boldsymbol{\xi}_{\text{lon}}^{\text{T}})^{j}\boldsymbol{P}_{\text{lon}}\boldsymbol{G}_{d\text{lon}} \quad j\geqslant 0 \tag{20}$$

where

$$\boldsymbol{\xi}_{\text{lon}}=\boldsymbol{\Phi}_{\text{lon}}+\boldsymbol{G}_{\text{lon}}\boldsymbol{F}_{k\text{lon}} \tag{21}$$

Eqs. (17)—(21) are substituted into Eq. (16), so optimal preview control law of longitudinal channel of carrier-based aircraft is

$$\boldsymbol{u}_{\text{lon}}(k)=\boldsymbol{F}_{ke\text{lon}}\frac{z}{z-1}\boldsymbol{e}_{\text{lon}}(k)+\boldsymbol{F}_{kx\text{lon}}\boldsymbol{x}_{\text{lon}}(k)-\boldsymbol{F}_{kx\text{lon}}\frac{z}{z-1}\boldsymbol{x}_{\text{lon}}(0)+\frac{z}{z-1}\boldsymbol{u}_{\text{lon}}(0)+\sum_{j=0}^{M_R}\boldsymbol{F}_{R\text{lon}}(j)\boldsymbol{R}_{\text{lon}}(k+j)+\sum_{j=0}^{M_d}\boldsymbol{F}_{d\text{lon}}(j)\boldsymbol{d}_{\text{lon}}(k+j) \tag{22}$$

where $\boldsymbol{F}_{k\text{lon}}=[\boldsymbol{F}_{ke\text{lon}} \quad \boldsymbol{F}_{kx\text{lon}}]$.

The first four terms of Eq. (22) are the feedback terms. The fifth term $\sum_{j=0}^{M_R}\boldsymbol{F}_{R\text{lon}}(j)\boldsymbol{R}_{\text{lon}}(k+j)$ is feed forward compensation term of the future reference information, and the sixth $\sum_{j=0}^{M_d}\boldsymbol{F}_{d\text{lon}}(j)\boldsymbol{d}_{\text{lon}}(k+j)$ is feed forward compensation term of the future disturbance information.

2.3 Lateral channel optimal preview control scheme

Discrete linear equations of lateral channel of carrier-based aircraft are

$$\begin{aligned}\boldsymbol{x}_{\text{lat}}(k+1)&=\boldsymbol{A}_{\text{lat}}\boldsymbol{x}(k)+\boldsymbol{B}_{\text{lat}}\boldsymbol{u}_{\text{lat}}+\boldsymbol{E}_{\text{lat}}\boldsymbol{d}_{\text{lat}}\\ \boldsymbol{y}_{\text{lat}}(k)&=\boldsymbol{C}_{\text{lat}}\boldsymbol{x}_{\text{lat}}(k)\end{aligned} \tag{23}$$

where $\boldsymbol{A}_{\text{lat}}$, $\boldsymbol{B}_{\text{lat}}$, $\boldsymbol{C}_{\text{lat}}$, $\boldsymbol{E}_{\text{lat}}$ are corresponding dimension matrices.

Liking longitudinal channel, lateral error signal is introduced

$$\boldsymbol{e}_{\text{lat}}(k)=\boldsymbol{R}_{\text{lat}}(k)-\boldsymbol{y}_{\text{lat}}(k) \tag{24}$$

where $\boldsymbol{R}_{\text{lat}}$ is the lateral reference value and $\boldsymbol{y}_{\text{lon}}$ the lateral output value.

Eq. (24) is substituted into Eq. (23), so a new state space equation is obtained

$$\begin{bmatrix} \boldsymbol{e}_{\text{lat}}(k+1) \\ \Delta \boldsymbol{x}_{\text{lat}}(k+1) \end{bmatrix} = \begin{bmatrix} \boldsymbol{I}_{\text{lat}} & -\boldsymbol{C}_{\text{lat}}\boldsymbol{A}_{\text{lat}} \\ 0 & \boldsymbol{A}_{\text{lat}} \end{bmatrix} \begin{bmatrix} \boldsymbol{e}_{\text{lat}}(k) \\ \Delta \boldsymbol{x}_{\text{lat}}(k) \end{bmatrix} + \begin{bmatrix} -\boldsymbol{C}_{\text{lat}}\boldsymbol{B}_{\text{lat}} \\ \boldsymbol{B}_{\text{lat}} \end{bmatrix} \Delta \boldsymbol{u}_{\text{lat}}(k) + \begin{bmatrix} \boldsymbol{I}_m \\ 0 \end{bmatrix} \Delta \boldsymbol{R}_{\text{lat}}(k+1) + \begin{bmatrix} -\boldsymbol{C}_{\text{lat}}\boldsymbol{E}_{\text{lat}} \\ \boldsymbol{E}_{\text{lat}} \end{bmatrix} \Delta \boldsymbol{d}_{\text{lat}}(k) \tag{25}$$

namely

$$\boldsymbol{X}_{\text{lat}}(k+1) = \boldsymbol{\Phi}_{\text{lat}}\boldsymbol{X}_{\text{lat}}(k) + \boldsymbol{G}_{\text{lat}}\boldsymbol{U}_{\text{lat}}(k) + \boldsymbol{G}_{R\text{lat}}\boldsymbol{R}_{\text{lat}}(k+1) + \boldsymbol{G}_{d\text{lat}}\boldsymbol{D}_{\text{lat}}(k) \tag{26}$$

Since reference value of lateral channel of carrier-based aircraft is zero, Eq. (26) can be expressed as

$$\boldsymbol{X}_{\text{lat}}(k+1) = \boldsymbol{\Phi}_{\text{lat}}\boldsymbol{X}_{\text{lat}}(k) + \boldsymbol{G}_{\text{lat}}\boldsymbol{U}_{\text{lat}}(k) + \boldsymbol{G}_{d\text{lat}}\boldsymbol{D}_{\text{lat}}(k) \tag{27}$$

The evaluation function of lateral channel is expressed as

$$\boldsymbol{J}_{\text{lat}} = \sum_{k=-M+1}^{\infty} [\boldsymbol{X}_{\text{lat}}^{\text{T}}(k)\boldsymbol{Q}_{\text{lat}}\boldsymbol{X}_{\text{lat}}(k) + \boldsymbol{U}_{\text{lat}}^{\text{T}}(k)\boldsymbol{H}_{\text{lat}}\boldsymbol{U}_{\text{lat}}(k)] \tag{28}$$

where $\boldsymbol{Q}_{\text{lat}}$ is a semi positive definite matrix and $\boldsymbol{H}_{\text{lat}}$ a positive definite matrix.

In order to get the minimum value of Eq. (28), the control input is

$$\Delta \boldsymbol{u}_{\text{lat}}(k) = \boldsymbol{F}_{k\text{lat}}\boldsymbol{X}_{\text{lat}}(k) + \sum_{j=0}^{M_d} \boldsymbol{F}_{d\text{lat}}(j)\Delta \boldsymbol{d}_{\text{lat}}(k+j) \tag{29}$$

where

$$\boldsymbol{F}_{k\text{lat}} = -[\boldsymbol{H}_{\text{lat}} + \boldsymbol{G}_{\text{lat}}^{\text{T}}\boldsymbol{P}_{\text{lat}}\boldsymbol{G}_{\text{lat}}]^{-1}\boldsymbol{G}_{\text{lat}}^{\text{T}}\boldsymbol{P}_{\text{lat}}\boldsymbol{\Phi}_{\text{lat}} \tag{30}$$

$$\boldsymbol{P}_{\text{lat}} = \boldsymbol{Q}_{\text{lat}} + \boldsymbol{\Phi}_{\text{lat}}^{\text{T}}\boldsymbol{P}_{\text{lat}}\boldsymbol{\Phi}_{\text{lat}} - \boldsymbol{\Phi}_{\text{lat}}^{\text{T}}\boldsymbol{P}_{\text{lat}}\boldsymbol{G}_{\text{lat}}[\boldsymbol{H}_{\text{lat}} + \boldsymbol{G}_{\text{lat}}^{\text{T}}\boldsymbol{P}_{\text{lat}}\boldsymbol{G}_{\text{lat}}]^{-1}\boldsymbol{G}_{\text{lat}}^{\text{T}}\boldsymbol{P}_{\text{lat}}\boldsymbol{\Phi}_{\text{lat}} \tag{31}$$

$$\boldsymbol{F}_{d\text{lat}}(j) = -[\boldsymbol{H}_{\text{lat}} + \boldsymbol{G}_{\text{lat}}^{\text{T}}\boldsymbol{P}_{\text{lat}}\boldsymbol{G}_{\text{lat}}]^{-1} * \boldsymbol{G}_{\text{lat}}^{\text{T}}(\boldsymbol{\xi}_{\text{lat}}^{\text{T}})^j\boldsymbol{P}_{\text{lat}}\boldsymbol{G}_{d\text{lat}} \quad j \geqslant 0 \tag{32}$$

$$\boldsymbol{\xi}_{\text{lat}} = \boldsymbol{\Phi}_{\text{lat}} + \boldsymbol{G}_{\text{lat}}\boldsymbol{F}_{k\text{lat}} \tag{33}$$

According to Eqs. (30)—(33), the control law is

$$\boldsymbol{u}_{\text{lat}}(k) = \boldsymbol{F}_{ke\text{lat}}\frac{z}{z-1}\boldsymbol{e}_{\text{lat}}(k) + \boldsymbol{F}_{kx\text{lat}}\boldsymbol{x}_{\text{lat}}(k) - \boldsymbol{F}_{kx\text{lat}}\frac{z}{z-1}\boldsymbol{x}_{\text{lat}}(0) + \frac{z}{z-1}\boldsymbol{u}_{\text{lat}}(0) + \sum_{j=0}^{M_d}\boldsymbol{F}_{d\text{lat}}(j)\boldsymbol{d}_{\text{lat}}(k+j) \tag{34}$$

Eqs. (22) and (34) are the same form because of the same algorithm. Since the longitudinal height is not zero while the lateral deviation is, there is a preview feed coefficient of target value in longitudinal channel.

3 Simulation

In order to verify the effectiveness of optimal preview control system, the control system is applied to the nonlinear model of carrier-based aircraft carrier landing.

3.1 Carrier landing simulation without initial deviation

First of all, all state variables and control inputs of carrier-based aircraft carrier landing are at equilibrium landing state. Initial height deviation and initial lateral deviation are all zero. Optimal preview controller and PID controller are compared in the same state. In the following charts, OPC denotes the optimal preview controller, PID the proportional integral differential controller and REF the reference height value in longitudinal channel or the reference lateral deviation in lateral channel.

Carrier-based aircraft tracks reference glide path, so height information which changes with time is very important.

According to Fig. 3, REF dynamic tracking performance of the height by OPC is more satisfied than that by PID.

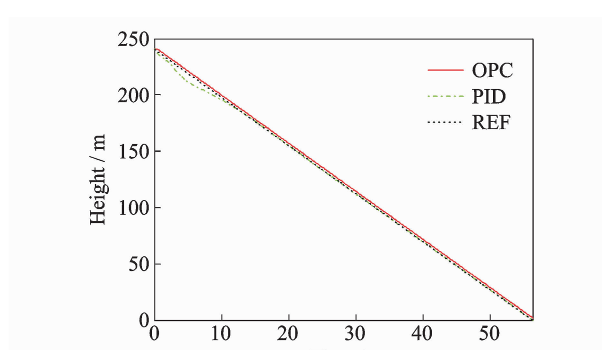

Fig. 3 Height comparison

According to Figs. 4, 5, it is shown that average height deviation of OPC is smaller than that of PID controller. Response speed of optimal preview controller is also relatively faster than that of PID controller.

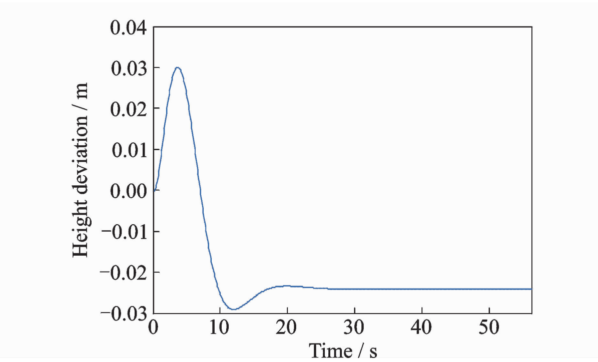

Fig. 4 OPC height deviation

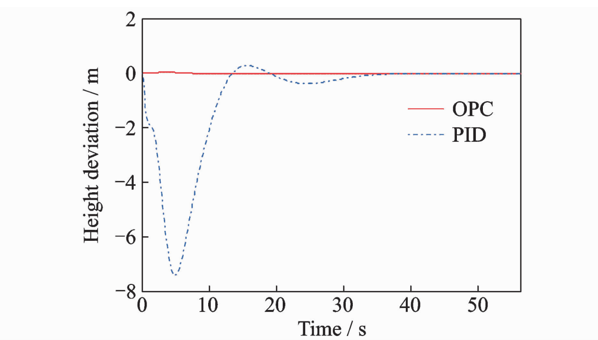

Fig. 5 Height deviation comparison

In the lateral channel, since initial deviation and equilibrium landing states are all zero, reference deviation, deviation of optimal preview controller and deviation of PID controller are all zero. Namely, result of optimal preview controller is equal to that of PID controller.

3.2 Carrier landing simulation with initial deviation

In practice there is a more or less deviation in initial location of carrier-based aircraft. In order to accurately reflect the situation results of carrier-based aircraft carrier landing, initial 10 m of deviation is added into the longitudinal channel and the lateral channel, respectively.

Simulation results of the height and the lateral deviation are shown in the following figures.

According to Figs. 6, 7, it is easily seen that height fluctuation of optimal preview controller is smaller than that of PID controller. OPC is stable at 22 s, but PID controller is stable at 35 s.

Figs. 6—8 show that dynamic performance of optimal preview controller is better than that of PID controller.

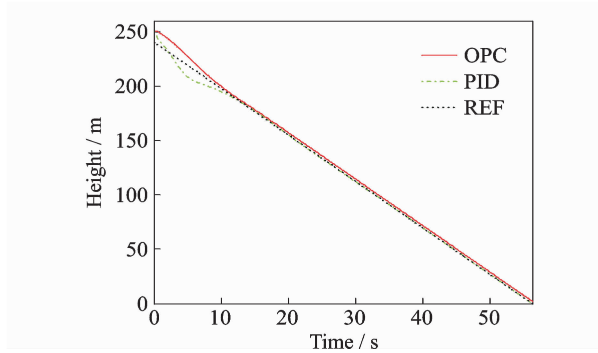

Fig. 6 Height comparison with initial 10 m deviation

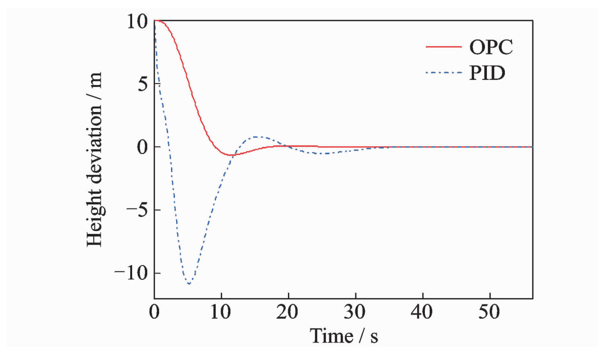

Fig. 7 Height deviation comparison with initial 10 m deviation

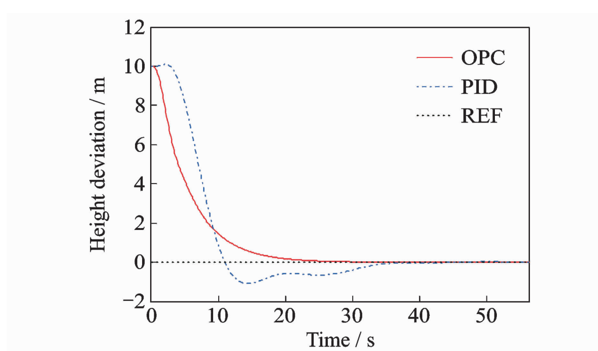

Fig. 8 Lateral deviation comparison with initial 10 m deviation

3.3 Carrier landing simulation with air wake

First of all, air wake is modeled, involving the influence for height and lateral deviation. Considering the actual carrier landing environment, air wake is added at 12.5 s before carrier landing.

In Figs. 9—11, FATC denotes the free atmospheric turbulence component; SSC the steady state component; PC the periodic component and RC the random component.

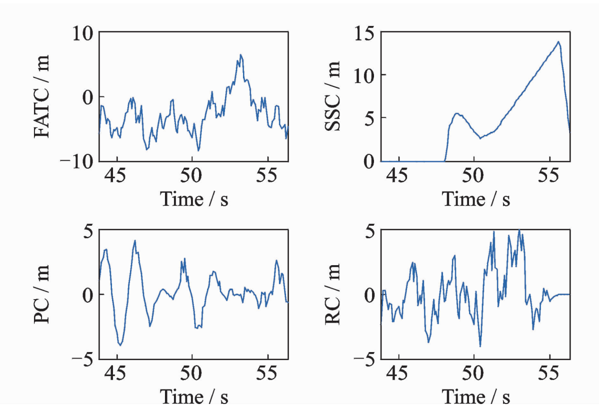

Fig. 9 Horizontal wake component

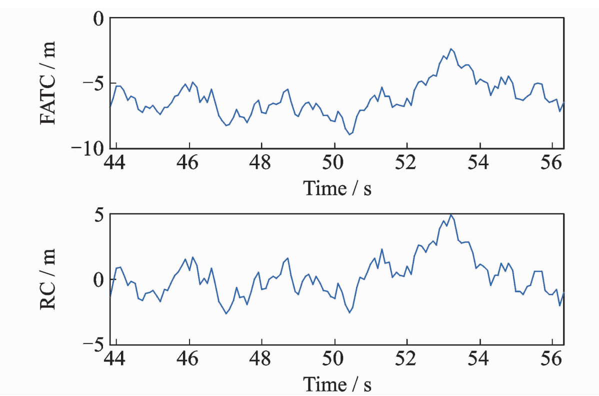

Fig. 10 Transverse wake component

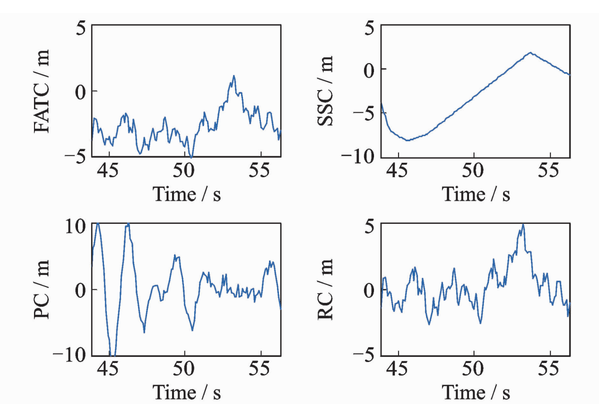

Fig. 11 Longitudinal wake component

Steady state component and periodic component are relatively significantly affected by sea state. Free atmospheric turbulence component and random component are generated by the atmosphere itself (Fig. 12).

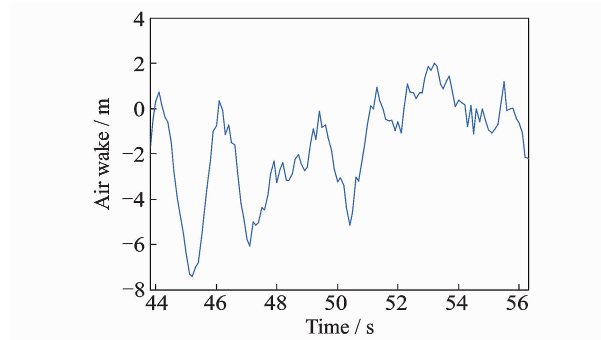

Fig. 12 Longitudinal air wake

The air wake is added into carrier landing process, and the height and the height deviation are shown below.

According to Figs. 13—15, optimal preview controller is better than PID controller in terms of response speed and fluctuation.

Lateral deviation is shown in Fig. 15 with air wake.

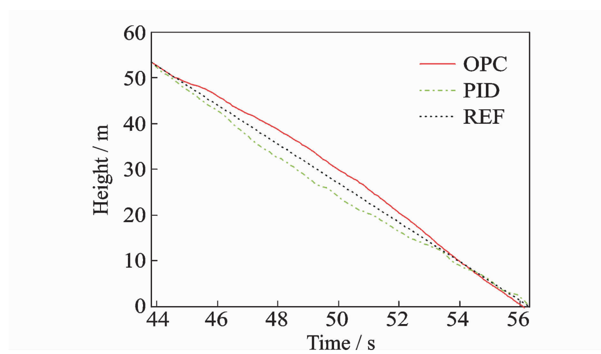

Fig. 13 Height comparison with air wake

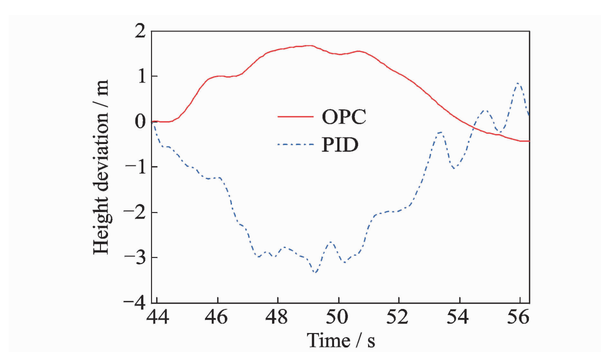

Fig. 14 Height deviation comparison with air wake

4 Conclusions

The optimal preview control scheme based automatic carrier landing system has been pro-

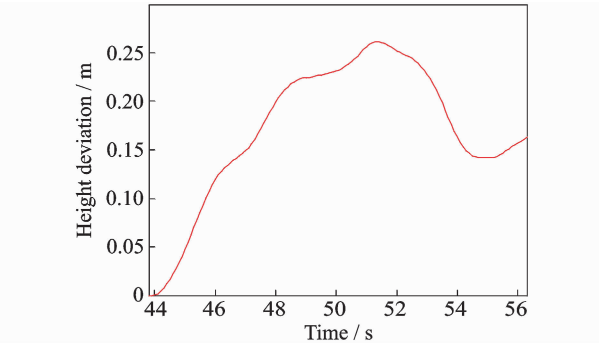

Fig. 15 Lateral deviation with air wake

posed for a six degree-of-freedom nonlinear carrier-based aircraft flight model with initial deviation and air wake. The carrier-based aircraft is to track reference glide path, so the optimal preview controller is designed. The simulation results show that optimal preview control algorithm is feasible for nonlinear model of carrier-based aircraft carrier landing. Dynamic performance index of carrier-based aircraft is also very good. Optimal preview controller is better than PID controller in stability and response speed with air wake and initial deviation.

Acknowledgments

This work was supported in part by the National Natural Science Foundation of China (Nos. 61741313, 61304223, 61673209, 61533008), the Jiangsu Six Peak of Talents program (No. KTHY-027), the Aeronautical Science Foundation (No. 2016ZA 52009), and the Fundamental Research Funds for the Central Universities (Nos. NJ20160026, NS2017015).

References:

[1] CHEN C, ZHOU R, WU H. Analyse of landing process of air wings based on cooperation with the carrier [J]. Computer and Information Technology, 2010, 4: 8-10.

[2] MOOK D J, SWANSON D A, ROEMER M J. Improved noise rejection in automatic carrier landing systems [J]. Journal of Guidance, Control, and Dynamics, 1992, 15(2): 509-519.

[3] NIEWOEHNER R J, KAMINER I I. Design of an autoland controller for a carrier-based F-14 aircraft using H∞ output-feedback synthesis[J]. American Control Conference, 1994, 3: 2501-2505.

[4] KAMINER I, KHARGONEKAR P P. Design of the flare control law for longitudinal autopilot using H∞ synthesis [C]// 29th IEEE Conference on Decision and Control, [S. l.]: IEEE, 1990: 2981-2986.

[5] KAMINER I, KHARGONEKAR P P, ROBEL G. Design of localizer capture and track modes for a lateral autopilot using H-infinity synthesis [J]. Control Systems Magazine, 1990, 10(4): 13-21.

[6] ZHU Q, YU Y, ZHANG W. Discrete variable structure control design for APCS of carrier-based aircraft based on dynamic disturbance compensation [C]// Industrial Engineering and Engineering Management, Changchun, China: IEEE, 2011: 1671-1675.

[7] ZHANG W, ZHANG Z, ZHU Q, et al. Dynamics model of carrier-based aircraft landing gears landed on dynamic deck [J]. Chinese Journal of Aeronautics, 2009, 22(4): 371-379.

[8] LI X, ZHAO T. Carrier-based aircraft landing process safety simulation analysis based on fuzzy inference [J]. Acta Aeronautica et Astronautica Sinica, 2013, 34(2): 325-333.

[9] TAKESHI T, TADASHI E. Newest auto control technique—digital preview control [M]. Beijing: Beijing Science and Technology Press, 1994.

[10] SHEN J, JIN L, CHEN L. Simulation study on load preview control system of a thermal power unit [J]. Journal of Chinese Electrical Engineering Science, 1999, 03:14-18,55.

[11] ZHEN Z, WANG Z, WANG D. Optimal preview tracking control based on information fusion in error system [J]. Control Theory & Applications, 2009, 4:425-428.

[12] ZHEN Z, WANG Z, WANG D. Preview control of discrete linear system based on information fusion estimation [J]. Acta Automatics Sinica, 2010, 2: 347-352.

[13] ZHEN Z. Research development in preview control theory and applications [J]. Acta Automatics Sinica, 2016, 2:172-188.

[14] CHEN Z, HAN W, CHEN J. Simulation of the longitudinal carrier landing in different sea-states for carrier-based aircraft [C]// International Symposium on Computational Intelligence and Design. Hang-

zhou, China: IEEE, 2015: 474-477.

[15] LI H, SU X, JIANG H. Modeling landing control system of carrier-based aircraft on internet of things [C]// Software Intelligence Technologies and Applications & International Conference, [S. l.]: [s. n.], 2014: 266-271.

[16] YANG Y. Carrier landing guide and control of carrier-based aircraft [M]. Beijing: National Defense Industry Press, 2007.

[17] ZHANG W, WANG X, LIU C. Study on automatic control system for longitudinal landing on carrier [J]. Journal of Northwestern Polytechnic University, 1996, 04:549-553.

Mr. **Li Meng** received his master degree in navigation guidance and control from Nanjing University of Aeronautics and Astronautics (NUAA), Nanjing, China, in 2017.

Dr. **Zhen Ziyang** received his Ph. D. degree in auto-control system from NUAA, Nanjing, China. He is now an associate professor and mainly researches automatic carrier landing system, unmanned aerial vehicle formation, preview control and adaptive control.

Prof. **Gong Huajun** received his Ph. D. degree in auto-control system from NUAA, Nanjing, China. He is now a professor and mainly researches flight control system.

Mr. **Hou Min** is a graduate student. His research focuses on UAVs' control.

Mr. **Huang Shuhong** received his master degree in navigation guidance and control from Nanjing University of Aeronautics and Astronautics (NUAA), Nanjing, China, in 2017.

(Executive Editor: Zhang Bei)